Precambrian Research 377 (2022) 106735

Contents lists available at ScienceDirect

Precambrian Research

journal homepage: www.elsevier.com/locate/precamres

Tectonic domains in the NW Amazonian Craton from geophysical and geological data

Ismael E. Moyano-Nieto[a,b,*], Germán A. Prieto[a], Mauricio Ibañez-Mejia[c]

[a] Departamento de Geociencias, Universidad Nacional de Colombia, Carrera 30 #45-03, Bogotá, Colombia
[b] Dirección de Recursos Minerales, Servicio Geológico Colombiano, Diagonal 53 #34-53, Bogotá, Colombia
[c] Department of Geosciences, University of Arizona, 1040 E 4th St., Room 208, Gould-Simpson Building, Tucson, AZ 85721, United States

ARTICLE INFO

Keywords:
NW Amazonian Craton
Magnetic/Gravity data interpretation
Geophysical/Geological data integration

ABSTRACT

The Amazonian Craton is one of the largest cratonic areas in the world. In Colombia, a major portion of the Craton is covered by Paleozoic to Cenozoic sedimentary rocks and recent deposits. This, in addition to the difficulty of access and dense tropical rainforest, have made the geology of this area to remain relatively unexplored to this date. Most accepted models for the Proterozoic evolution of the Amazonian Craton indicate that it evolved via successive accretion of orogenic belts and crustal terranes around an ancient nucleus, and that tectonic provinces identified in the southern half of the craton, the Guaporé Shield, extend underneath the Amazon River Basin onto its northern exposure, the Guiana Shield. Nevertheless, recent geologic studies in the W Guiana Shield indicate that its evolution may have been different from the W Guaporé Shield, where these accretionary models were formulated. In this work, we used airborne gravity/magnetic geophysical datasets covering the NW portion of the Amazonian Craton, to better elucidate its structure and tectonic evolution. We apply a multiscale edge detection and 3D modeling to identify and delineate major crustal discontinuities and other geological features. Using this approach, we identified six primary geophysical lineaments that are interpreted as possible crustal boundaries. By combining our geophysical interpretation with all the geological, geochronologic and isotopic information available for the region, we propose the presence of the following tectonic domains: Ventuari-Tapajós, Rio Negro-Juruena (which we further subdivide into Atabapo and Vaupés Belts), Apaporis Graben, and Putumayo. Furthermore, a new U-Pb zircon crystallization age of 1227 ± 8/13 Ma obtained from volcanic rocks of the Piraparaná Formation indicates that extensional tectonics along the Apaporis Graben began at least in the late-Mesoproterozoic. This is significantly older than previously thought, and thus entirely transforms the tectonic significance of the Apaporis Graben structures. Our interpretation of structural limits is in excellent agreement with and provides a more accurate location for previously suggested boundaries, which were until now only loosely constrained by the sparse geological and geochronologic information available. This work provides the first regional reconstruction of crustal-scale features of NW South America, improving the understanding of the regional tectonic architecture of NW Amazonian Craton using geophysical methods.

1. Introduction

The Amazonian Craton forms part of the crystalline core of the South American continent and is divided by the Amazon River basin into two parts: the Guiana Shield in the north, and the Guaporé or Central Brazilian Shield in the South (Almeida, et al., 1981). It is also considered one of the largest cratonic areas in the world (Tassinari and Macambira, 1999), and is thought to have played a key role in the assembly and evolution of Precambrian supercontinents (Cordani et al., 2009). In Colombia, NW South America, rocks of the Amazonian Craton extend from the Andean deformation front to the borders with Venezuela and Brazil (Ibañez-Mejia and Cordani, 2020), covering an area of nearly 600,000 km^2. Nevertheless, most of the Amazonian Craton in this area is covered by Paleozoic to Cenozoic sedimentary rocks and recent deposits (Gómez et al., 2015; Gómez et al., 2019), and basement exposures are limited to remote regions near the borders between Colombia, Brazil and Venezuela, and as isolated basement outcrops located in the central part of the area (Fig. 1).

The geology of the NW portion of the Amazonian Craton, mainly in NW Brazil and E Colombia, remains relatively unexplored (Ibañez-Mejia

* Corresponding author.
E-mail address: iemoyanon@unal.edu.co (I.E. Moyano-Nieto).

https://doi.org/10.1016/j.precamres.2022.106735
Received 10 November 2021; Received in revised form 13 May 2022; Accepted 13 May 2022
Available online 1 June 2022

and Cordani, 2020; Santos, et al., 2000). Dense rainforest coverage, lack of roads, and difficult access to where basement rocks are exposed, make this region one of the largest and least known domains of Archean-Proterozoic crust in the world.

At least two models for the evolution of the Amazonian Craton indicate that it evolved by multiple episodes of accretion of island arcs around an Archean nucleus (Barrios, et al., 1985; Tassinari and Macambira, 1999; Santos et al., 2000; Cordani and Teixeira, 2007; Brito, 2011; Ibañez-Mejia et al., 2011; Kroonemberg, 2019). However, recent studies (Ibañez-Mejia et al., 2015; Cordani et al., 2016a; Ibañez-Mejia and Cordani, 2020) have observed that the geological evolution of the W Guiana Shield may have been different compared to the W Guaporé Shield, where the Mesoproterozoic Rio Negro-Juruena, Rondonian-San Ignacio, and Sunsás-Aguapei provinces were defined (Tassinari et al., 1996; Bettencourt et al., 2010; Teixeira et al., 2010).

Geophysics aims to image subsurface geological structures that are not directly observable in the field and is fundamental in the identification of otherwise cryptic geologic features (Li, et al., 2019). Geophysical methods are sensitive to differences in the physical properties of rocks (Dentith and Mudge, 2014), such as density (via gravimetry) and magnetic susceptibility (via magnetometry). Interpretation of gravity and magnetic data have been successfully applied for understanding basement structures and boundaries in other poorly exposed, buried, or densely vegetated regions of the South American basement (e.g., De Castro et al., 2014; Pessano et al., 2021), and on other cratonic areas of the world (Heath, et al., 2009. Crawford, et al., 2010).

The integration of geophysical data such as airborne gravity and magnetic measurements enhances and extend the geological information observed in the field (Isles and Rankin, 2013). These geophysical methods provide a nearly homogeneous coverage of the variations in gravity and magnetic properties over large areas, which in turn allow changes in the density and magnetic susceptibility of rocks in the upper crust to be identified and delineated (Isles and Rankin, 2013; Jacoby and Smilde, 2009).

In the present work, qualitative and quantitative interpretation of the available geophysical (magnetic and gravity) datasets, along with available geochronologic information, are used to propose an integrated geophysical-geological model for the NW portion of the Amazonian Craton in E Colombia. From this geological-geophysical integration, we identify major structural/tectonic boundaries and propose a subdivision into five tectonic domains, each one of these with its own structural and geological characteristics. Our observations and interpretation of the available geophysical data provide: i) a regional model of the tectonic framework and evolution of the NW Amazonian Craton that is informed by, and is coherent with, all available geologic and geochronologic data; and ii) new insights into the geological evolution of this poorly known region of the South American Precambrian basement.

2. Regional geology

The Amazonian Craton in Colombia extends from the eastern flank of the Andean Cordillera to the borders with Venezuela, Brazil, and Peru (Fig. 1a). The westernmost part of this region corresponds to the Llanos foothills area, where the craton is buried under a thick sedimentary cover of the foreland Caguán-Putumayo and Llanos basins (Ibañez-Mejia and Cordani, 2020). Exposures of the Amazonian Craton represent only ~ 10 % of the whole area and are concentrated to the east in the border with Brazil and Venezuela (Fig. 1b). The westernmost exposures are in the Araracuara high along the Caquetá River (Gómez et al., 2015). Also, drill-core samples from wells in the Putumayo Basin near the Andean deformation front (Ibañez-Mejia et al., 2011) demonstrated the continuity of the Craton under the sedimentary cover. Note that, throughout this paper, all discussions about the ages of particular units or events refer to values obtained using U-Pb zircon geochronology unless otherwise noted. For more details about the methods (e.g., LA-ICPMS, SIMS, TIMS) the reader is referred to the Supplementary Materials and the original geochronologic studies cited throughout the text.

In Colombia, the Amazonian Craton is characterized by Paleoproterozoic (1.5 to 1.9 Ga) gneisses, amphibolites, migmatites, quartzites, and granitoids grouped as the Mitú Migmatitic Complex (Galvis et al., 1979; Gómez et al., 2015) or Mitú Complex (Celada et al., 2006; Rodríguez et al., 2010; López et al., 2010; Ibañez-Mejia and Cordani, 2020). The highly deformed and metamorphosed units of the Mitú Complex are intruded by moderately deformed to undeformed Mesoproterozoic granitoids, some of them with Rapakivi texture such as the Parguaza Granite (ca. 1.4 Ga), located within Venezuela and Colombia, and that is considered one of the largest anorogenic intrusions of the world (Bonilla-Perez et al., 2013). In some areas, the Mitú Complex is

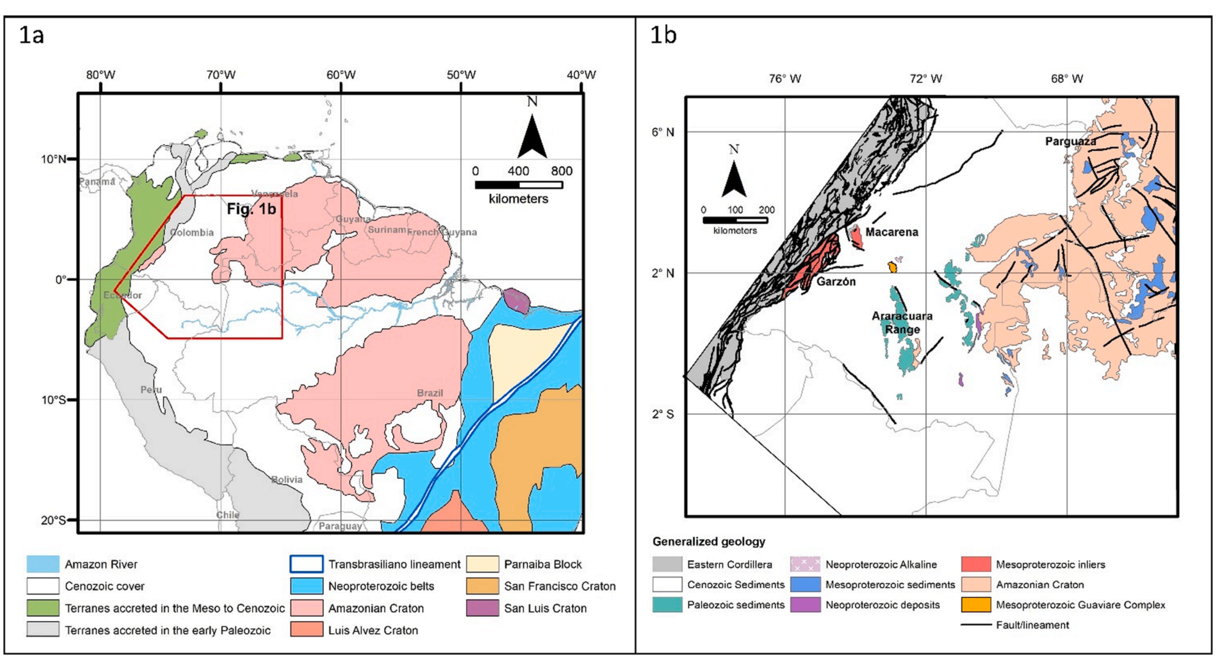

Fig. 1. a: Regional extent and geotectonic framework of the Amazonian Craton (Modified from Cordani et al., 2016b). b: Location and regional geology of the study area (Modified from Gómez et al., 2015; Gómez et al., 2019 and Amaya López et al., 2020).

overlain by Mesoproterozoic low-grade metasedimentary rocks of the La Pedrera formations (Gómez et al., 2015), the Tunuí Group (Kroonemberg, 2019), volcano-sedimentary rocks of the Piraparaná Formation, and Ediacaran through Carboniferous marine sedimentary rocks. These exposures form isolated hills and Tepuis over the flat landscape of the area.

Amaya López et al. (2020) presented evidence of Mesoproterozoic (1.3 Ga) crust in the central part of the area, near San José del Guaviare (Fig. 1b). According to these authors, rocks of the Guaviare Complex originated as part of bimodal magmatism on an extensional environment associated with arc extension. The 1.3 Ga magmatism as described in the Guaviare Complex is younger than the Mitú Complex and had not been previously recognized in other outcrops of the Amazonian Craton in Colombia. Younger magmatism on the Amazonian Craton is represented by mafic intrusives and dikes of 1.18–1.22 Ga Rb/Sr ages (Priem et al., 1982), 973 Ma (Caño Viejita gabro; Bonilla et al., 2020), and 826 Ma K/Ar age (Vaupés 1 well) (Franks, 1988 in: Kroonemberg, 2019). Alkaline plutons of 621–634 Ma and 577.8 Ma are present in the northeastern flank of the Serranía de la Macarena (Caño Veinte syenite; Buchely et al., 2015) and in San Jose del Guaviare (San José nepheline syenite; Amaya López et al., 2021), respectively. A Cretaceous (102.5 Ma) diabase was discovered on the Caquetá River near the Serranía de Araracuara by Ibañez-Mejia and Cordani (2020).

2.1. Structural features

Structural data presented in geological maps by the Colombian Geological Survey, east of the Andean deformation front, are scarce (Fig. 1b; see Gómez et al., 2015; Gómez et al., 2019). In Colombia, faults and lineaments with predominant NW-SE (Carurú and Central Guainía lineaments, Puerto Colombia Fault) and NE-SW (Mitú, Cuiarí River, Caño Garza and Caño Chaquita faults, Papunaua Lineament) trends have been delineated. The N-S trending Naquén and Río Aque faults, that limit the Serranía de Naquén, are also identified. In the Venezuelan area (Hackley et al., 2005), the structural features identified are more abundant and with the same NW-SE and NE-SW trends identified in Colombia.

Regional structural models of the Amazonian Craton in Colombia are based on radar (De Boorder, 1981) and geophysical datasets integrated with available geological data (Etayo et al., 1983; Kroonemberg and De Roever, 2010; Kroonenberg and Reeves, 2012; De Boorder, 2019, Cediel, 2019; Moyano, et al., 2020). Fig. 2a shows the structures interpreted in the geological terrains map of Colombia (Etayo et al., 1983). The main structural feature in this map is the NW-SE "Apaporis rift", which is bound by NW-SE trending outcrops of Paleozoic strata and a NWW-SEE structure, the Carurú Fault, that limits the Apaporis Rift to the north and extends from the Serranía de la Macarena near the Andean foothills to Brazil. Another salient feature in Fig. 2a is a NE-SW structure south of the Carurú fault, known as the "La Trampa Rift" (Etayo, et al., 1983, Cediel, 2019) or "La Trampa Wedge" (De Boorder, 1981; Kroonenberg and Reeves, 2012; De Boorder, 2019). Fig. 2b shows a simplified map modified from Cediel (2019) that includes similar structures such as the "La Trampa Wedge" and a series of NW-SE lineaments that delineate the "Guejar Impactogen" ("Apaporis Rift" in Fig. 2a). This interpretation does not include the NW-SE Carurú fault. Regional faults highlighted by the Cediel (2019) model include the NWW-SEE Caquetá Fault south of the Paleozoic Araracuara range (approximately at 2°S) and the NEE-SWW Guaviare Fault (4°N) at the northern limit of the exposures of the Amazonian Craton in Colombia.

2.2. Geochronological provinces

Geochronological subdivisions for the evolution of the NW portion of the Amazonian Craton in Colombia have been proposed by Tassinari and Macambira (1999), Santos et al. (2000), Kroonemberg (2019), Ibañez-Mejia et al. (2011), and Ibañez-Mejia and Cordani (2020). Due to the limited geological and geochronological information for the area, and the extensive coverage with rainforest and sediments, tectonic boundaries and even the existence of specific basement domains remain debated. Despite these differences, there is general agreement that the craton in this region grew by continued collision/accretion of orogenic belts along the western margin of an early Paleoproterozoic cratonic nucleus established after the Transamazonian Orogeny (Ibañez-Mejia and Cordani, 2020). This process, driven by subduction-related processes, began at ca. 2.0 Ga and is thought to be responsible for the formation/accretion of the Ventuari-Tapajós, Rio Negro-Juruena, and Rondonian-San Ignacio provinces (Cordani and Teixeira, 2007).

Recent geochronological interpretations on the Amazonian Craton in Colombia and neighboring areas (Cordani et al., 2016a; Ibañez-Mejia and Cordani, 2020) proposed the existence of two possible orogenic belts within the Rio Negro-Juruena Province, namely the Atabapo (1.84–1.72 Ga) and Vaupés (1.59–1.50 Ga) belts. Also, these studies concluded that there is currently no geochronological data to support the presence of the Rondonian-San Ignacio province in the Guyana Shield as defined in NW Brazil and Bolivia (Ibañez-Mejia and Cordani, 2020), and that the Nd-Hf isotopic nature of the basement in Colombia

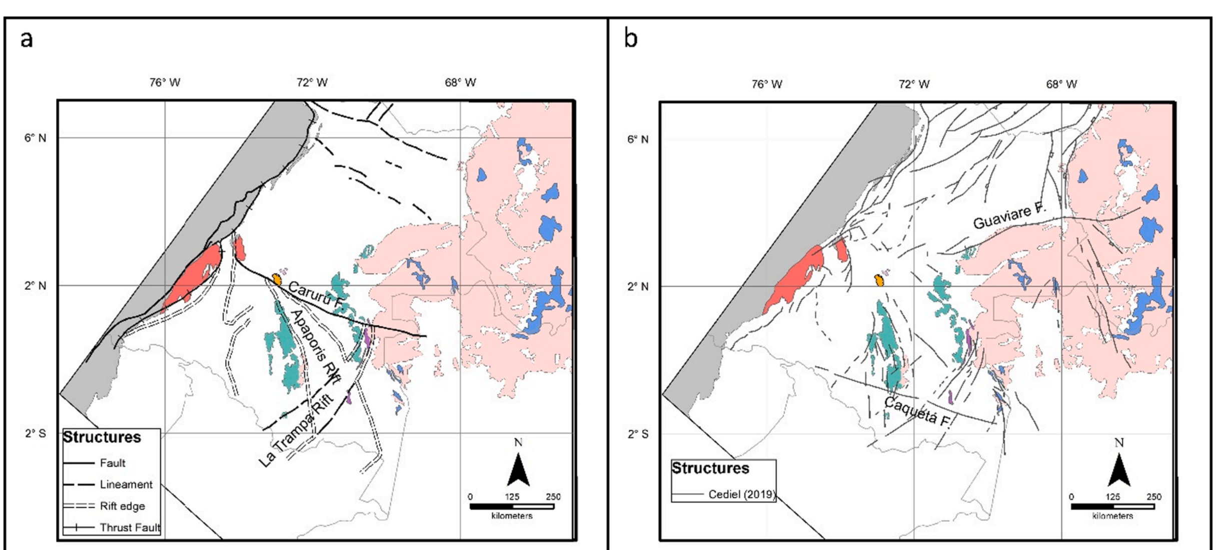

Fig. 2. Regional geology presented in Fig. 1 and structural intepretations from: (a) Etayo et al. (1983) and (b) Cediel (2019). Green: Paleozoic strata.

and Western Venezuela indicates a greater degree of older Paleoproterozoic crustal reworking relative to the correlative, more juvenile magmatic domains south of the Amazon River basin. The work of Bonilla et al. (2021), on the other hand, proposed a different geologic and tectonic history for the NW Amazonian Craton in the eastern Colombia basement. The authors concluded that the metamorphic basement in this region corresponds to the Rio Negro Belt (Rio Negro-Juruena province) built at the Querarí orogeny, and that the younger magmatism at 1.6–1.5 Ma and 1.4–1.3 Ma are related to post-orogenic to anorogenic stages of the same orogeny.

From the summary presented above, we can conclude there is general agreement in some elements characterizing the tectonic history of the NW Amazonian Craton, such as the presence and general location of the suture between the Rio Negro belt/ Rio Negro-Juruena province and the Ventuari-Tapajós province. In contrast, based on nearly the same geological and geochronological information, other elements such as the tectonic evolution of the Rio Negro-Juruena basement and the presence/ location of boundaries with younger geochronological provinces or terranes to the west is still under debate.

In order to resolve this debate, a clearer identification of the major crustal boundaries that separate geological terranes in the region is key, as this will allow better correlations with potentially correlative boundaries identified in the southern portion of the craton, as well as allow for improved paleogeographic reconstructions with other Precambrian cratons (Ibañez-Mejia and Cordani, 2020).

3. Methods

3.1. Geophysical data processing and interpretation

Lateral variations of the Earth's gravitational and magnetic fields over a region provide estimates of the distribution of physical properties (density and magnetic susceptibility) in the crust and upper mantle (Isles and Rankin, 2013; Jacoby and Smilde, 2009). Airborne geophysical data can provide coverage in large areas, which combined with field observations can greatly enhance our ability to identify structural/tectonic boundaries, particularly in regions were rock exposure is limited.

Here, we use a multiscale edge detection method or "worming" (Horowitz et al., 2000; Heath et al., 2009), integrated with qualitative data interpretation and 3D modelling, to define regional structural boundaries in our study area. Worming is based on the detection and delineation of the edges of the sources of gravity and magnetic anomalies at multiple upward continuation levels. Integration of the edges at multiple scales constraints the position and vertical continuity of major geological structures. Details on data processing and case studies can be found in Moyano and Prieto (2021) and references therein.

An example of successful application of multiscale edge detection was presented by Horowitz et al. (2000). The authors applied multiscale edge detection on EGM96 global geodetic gravity field, and the "worms" generated allowed to correlate global-scale tectonic boundaries like the subduction zone in Western South America. Crawford et al. (2010) applied worming on gravity and magnetic data across the western Australian Craton (Western Australia) and identified four major orogen parallel features interpreted as major faults and/or shear zones that extend to significant crustal depths. The authors interpreted these features to be related to more 'primary' cratonic margin structures at depth. In another example, Yan et al. (2011) applied worming on gravity and magnetic data on the Yangtze River metallogenic belt (China). The edges interpreted from worming allowed to interpretate the Yangtze River deep fault as a rift-valley-type fault caused by mantle upwelling, and to delineate the fault system that controls the upward migration of mineralized fluids and emplacement of known mineralized zones in the area.

3.2. Source of geophysical datasets

Continental-scale gravity and magnetic datasets from EIGEN-6C4 (Förste et al., 2014) and EMAG2-V3 (Meyer, et al., 2017), and regional airborne/ground surveys compiled for the National Hydrocarbon Agency of Colombia (ANH) (Graterol and Vargas, 2010) were integrated to generate full coverage (2.5 km grid size) Bouguer anomaly (BA) and Total Field anomaly (TFA) grids for the study area. Additionally, more detailed (500 m grid size) airborne magnetic datasets for eastern Colombia from the Geological Survey of Colombia (Moyano et al., 2018), and NW Brazil (ENCAL, 1988) were used (Fig. 3).

3.3. Multiscale edge detection

Semi-quantitative interpretation of the gravity and magnetic data of Fig. 4a and 4b used the multiscale edge detection procedure described by Heath et al. (2009). For this study we used upward continuation levels of the potential field data to 2, 4, 8, 16, 32, and 64 km. The total horizontal gradient of each upward continued image was calculated, and points of maximum slope were delineated following the method of Blakely and Simpson (1986). The edges at each continuation level were integrated in a single map for each geophysical method (Fig. 4a and 4b) allowing the identification of structures that, by its coherence in multiple upward continued levels, suggest deep-crustal penetrating features. Details on the orientation and correlation of the main geophysical features will be presented next. Also, it must be noted that each upward continuation level doesn't represent a specific depth (Heath et al., 2009).

3.4. U-Pb (LA-ICP-MS) zircon geochronology

Zircon crystals were concentrated using traditional magnetic and density separation techniques. Individual grains were hand-picked under a binocular microscope, mounted in epoxy resin, and polished to expose the interior of the grains prior to analysis. U-Pb geochronologic determinations were conducted by laser ablation–inductively coupled plasma–mass spectrometry (LA-ICP-MS) at the Arizona LaserChron Center (ALC), using a Photon Machines Analyte G2 laser coupled to a Nu Plasma multicollector ICP-MS. Instrumental bias, drift, and inter-element fractionation corrections were performed by the standard-sample bracketing (SSB) approach, using an in-house Sri Lanka zircon crystal with well-established ID-TIMS age of 563.5 ± 3.2 Ma as primary reference material. U-Pb analyses were performed using a laser-beam diameter of 30 μm and simultaneously measuring all Pb masses in Faraday cups. Data collection, processing, and uncertainty calculations follow the approach of Ibañez-Mejia et al. (2014). Mean dates discussed throughout the text are weighted mean $^{207}Pb/^{206}Pb$ values, and uncertainties are presented in the form ±X/Y, where X is solely analytical uncertainty, and Y is the total uncertainty that combines the analytical uncertainty, uncertainty in the ID-TIMS date of the primary reference material, SSB normalization uncertainty, and ^{238}U decay constant uncertainty.

4. Results

4.1. Major structural features from geophysical data interpretation

According to the authors and case studies referenced above (Horowitz et al., 2000; Crawford et al., 2010; Yan et al., 2011; and references therein), we consider the features highlighted by the worming of the gravity and magnetic data, that show continuity in multiple continuation levels, as deep penetrating linear structures that represent major crustal discontinuities. The discontinuities that show coherence and delineate lateral variations in both gravity and magnetic data, thus reflecting major lateral density and/or magnetic susceptibility variations in the upper crust, were identified in Fig. 5 as primary geophysical

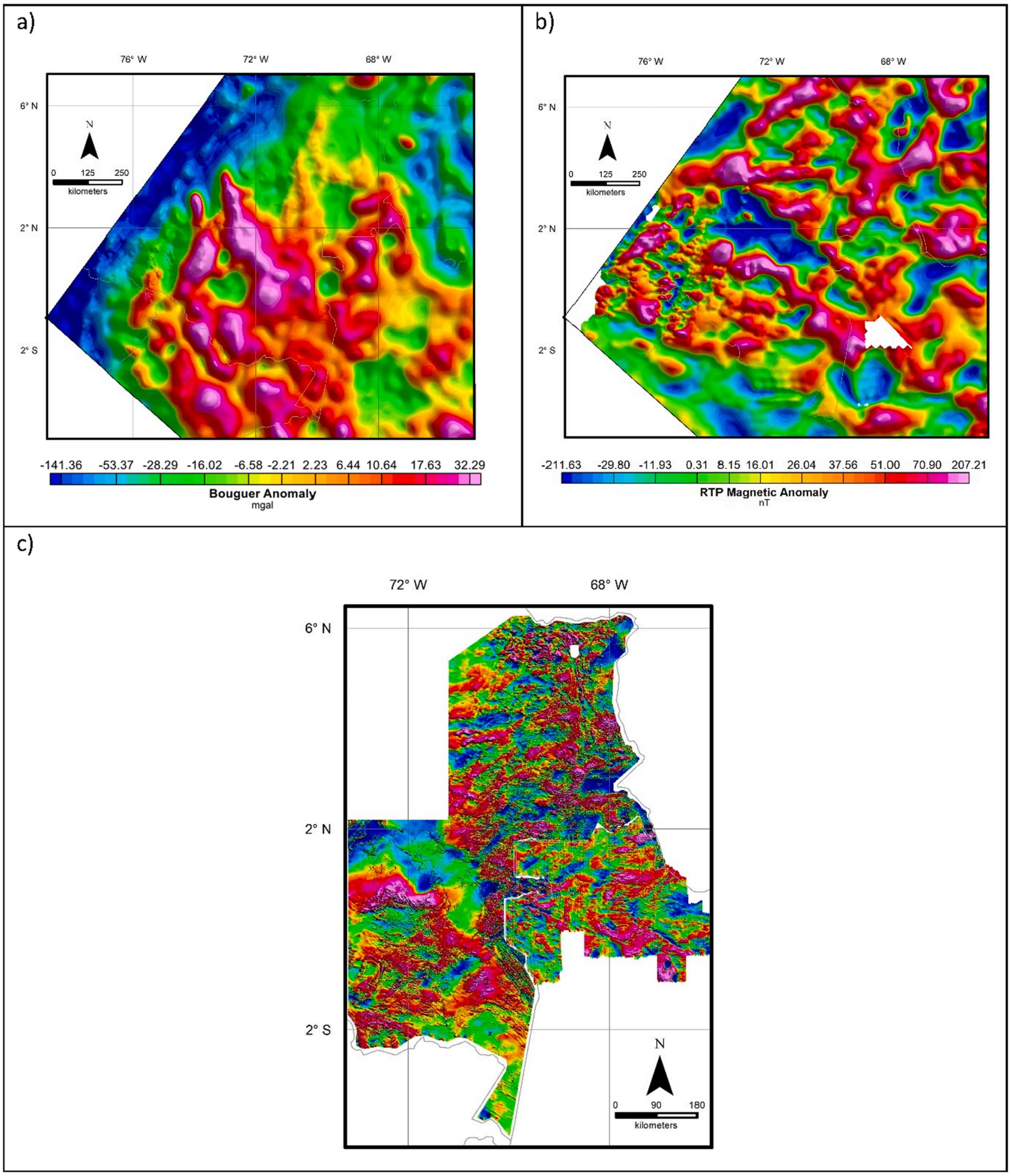

Fig. 3. (a) Bouguer anomaly (2.5 km grid size). (b) Magnetic Anomaly Reduced to Magnetic Pole (2.5 km grid size). (c) More detailed (500 m grid size) Magnetic Anomaly Reduced to Magnetic Pole.

lineaments (PGL; bold black lines). Other geophysical features that also show clear correlation in both geophysical datasets and related in its extension and orientation with the PGL, were identified as secondary geophysical lineaments (SGL; thin dashed lines).

Six PGL were identified (Fig. 5): PGL1 is a prominent SW-NE feature that is located along the western end of our study area. The remaining structures, PGL2 through PGL6, have predominant NW-SE orientation. Except for PGL4, which terminates to the NW against PGL3, all other geophysical lineaments (SGL included) are truncated to the NW by PGL1. These cross-cutting relationships between primary geophysical structures are particularly important because they provide information about the relative timing of each feature and hence on the geological/tectonic history of the area: PGL1 truncates PGL2, PGL3, PGL5, and PGL6, so it is most likely younger. Similarly, PGL3 cross-cuts PGL4, and thus the latter must be older.

The orientation and extent of secondary lineaments (SGL) in relation with our interpreted PGL are also of interest. West of the PGL1, secondary lineaments are scarce but with the same NE-SW trend. Between PGL2 and PGL3, secondary lineaments have NNE-SSW and NW-SE orientation and terminate against these primary lineaments. Between PGL4 and PGL5, secondary lineaments are sub-parallel to these primary structures, and also delineate a characteristic NW-SE low magnetic anomaly (Fig. 5b). The area comprised between PGL5 and PGL6 exhibits NNE-SSW and E-W structures that are also truncated by the primary structures.

Similarly to previous studies (Horowitz et al., 2000; Crawford et al., 2010; Yan et al., 2011), we interpret the geophysical features delineated by multiscale edges as deep crustal penetrating geological features.

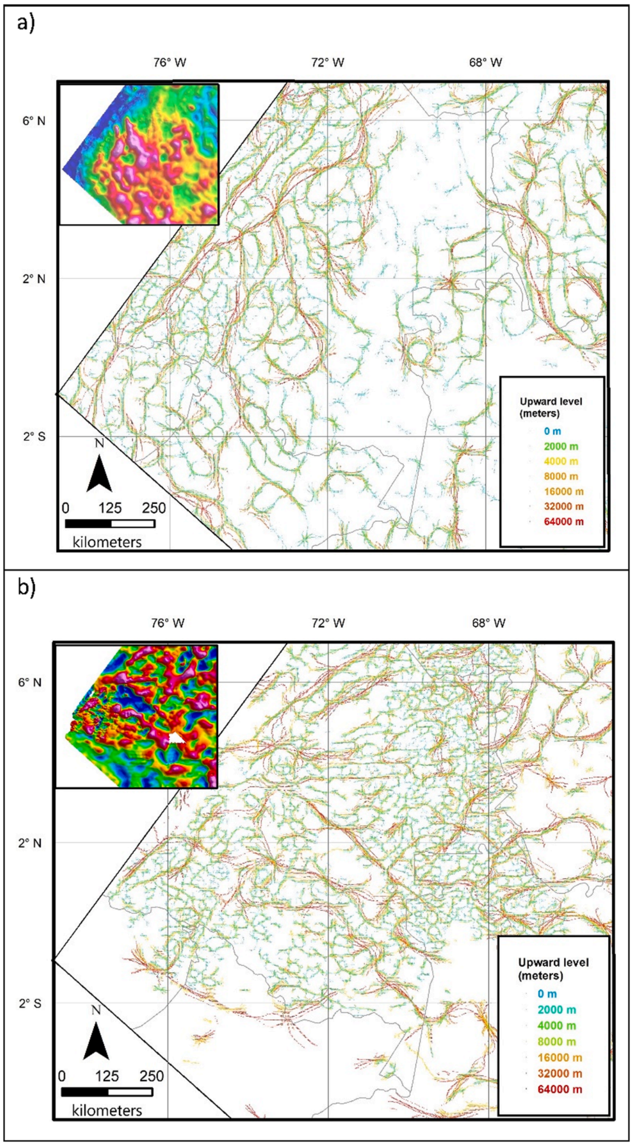

Fig. 4. Multiscale Edge detection applied to (a) Bouguer anomaly and (b) Magnetic anomaly reduced to magnetic pole.

Their spatial distribution and cross-cutting relationships as described above can also help to better constrain tectonic domains. The features presented in Fig. 5 suggest that the extension of the SGL are limited by the features interpreted as PGL, and that the general orientation of these SGL change from one PGL to another. We interpret the clustering of the structural pattern and distribution of the secondary geophysical features as possible "blocks" with different geological significance, and probably tectonic history. The PGL then could be interpreted as major crustal features that could be considered as tectonic boundaries (Horowitz et al., 2000; Heath et al. 2009, Fitzgerald and Milligan, 2013).

4.2. 3D inversion of potential field data

The cross sections indicated in Fig. 5b were used to integrate the geophysical interpretation with available geological data. To provide a quantitative view of the lateral and depth variation on the physical properties (density, magnetic susceptibility), 3D inversions on a strip along each section were computed. The 3D inversion routine used unconstrained density and Magnetic Vector Inversion (MVI; see MacLeod and Ellis, 2013) algorithms. For each Section indicated in Fig. 5, a mesh with 5000x5000x500 m cell size and 50 km depth were constructed. Figs. 6 and 7 show cross sections of the calculated magnetic susceptibility and density models along the selected profiles.

Cross Section 1 (Fig. 6) extends from SW of the Araracuara Range to the NE. The magnetic model (Fig. 6a) shows clear and sharp crustal discontinuities on the location of the PGL4, PGL5, and PGL6. Between PGL4 and PGL5, there is a low magnetic susceptibility zone near the surface that corresponds with the NW-SE magnetic low evidenced in the magnetic anomaly (Fig. 5b). This low magnetic susceptibility can be related with a basin filled with less magnetic sediments. The density model (Fig. 6b) also shows lateral variation associated with the primary geophysical structures. Both models show coherence between high/low density and high/low magnetic susceptibility zones that probably reflect variations in the composition of basement rocks. Examples of this correlation are high magnetic susceptibility and high-density sources around PGL4 and PGL5 and a large feature with high magnetic susceptibility and low density located to the NE of structure 6.

Cross section 2 (Fig. 7) extends from the Garzón Massif to northeasternmost Colombia (i.e., Vichada Region). Magnetic susceptibility and density models (Fig. 7a and 7b) show lateral variations correlated with PGLs 1,3,5, and 6. As also observed in cross section 1, there are correlations between density and magnetic susceptibility sources that probably reflect variation in the composition of the basement rocks, like the high magnetic susceptibility/low density source between PGL1 and PGL3, and the low density/magnetic susceptibility source to the SW of PGL6, contrasting to the moderate magnetic susceptibility/high density source to the NE. Another example of this correlation is the high magnetic susceptibility and low-density source located right in between PGL3 and PGL5, that corresponds to the exposure of the Guaviare Complex.

5. Integration with other geological information

From our interpretation of the geophysical data and inversions presented above, we argue that: i) crustal-scale structural features/domains can be identified; and ii) that these structures correlate with major tectonic boundaries characterizing the evolution of the NW Amazonian Craton basement, and that are supported by the existing field and geochronologic data.

The integration of our geophysics-based interpretation with available geological information allows us to better interpret the tectonic significance of the structural limits identified in our study region (Fig. 8). Each domain is characterized by its own geophysical properties and by geological and geochronological features that will be discussed (from older to younger) below. We also provide a supplementary Figure (S1) and Table (ST1) with number, rock type, age, analytical method, and references of the 62 samples included in Fig. 8.

It is important to highlight that the proposed tectonic domains correspond mainly to the delineation and interpretation of regional, crustal-scale geophysical boundaries that reflect lateral changes in the structure and/or physical properties of the upper crust. Our proposed tectonic domain model is in good agreement with the available geological and geochronological data and, as a model, provides hypotheses that should continue to be tested and improved upon as more petrophysical, geological, and geochronological data become available from this poorly studied region.

5.1. Ventuari-Tapajós tectonic domain

Located to the east of PGL6. Basement rocks in this domain are identified as Paleoproterozoic units of the Cuchivero Group, San Carlos metamorphic-plutonic terrane and Basement Complex (Hackley et al., 2005), and Mesoproterozoic intrusions like the Parguaza Granite. The Cuchivero Group represent an association of calc-alkaline granite-gneisses and volcano-sedimentary sequences with U/Pb and Rb/Sr ages of 1.98–1.83 Ga (Teixeira et al., 2002). Tassinari and Macambira (1999) interpreted this units as part of the 1.95–1.8 Ga Ventuari-Tapajós

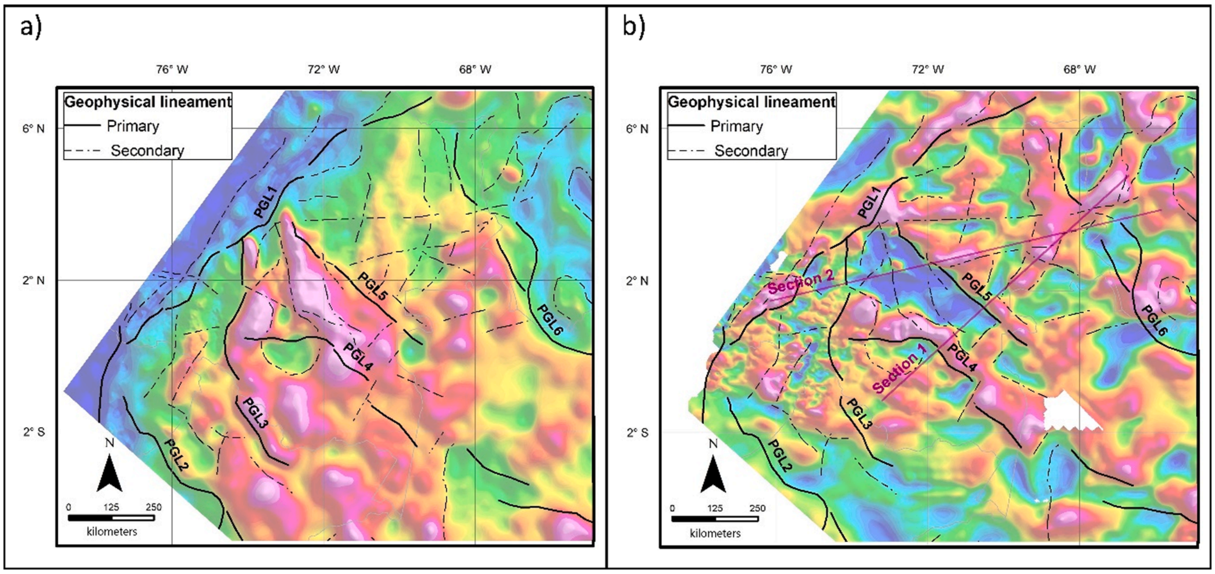

Fig. 5. Primary (PGL) and secondary (SGL) geophysical lineaments interpreted for the study area superimposed to gravity (a) and magnetic (b) data. (b) also show the location of the cross sections used to integrate the data.

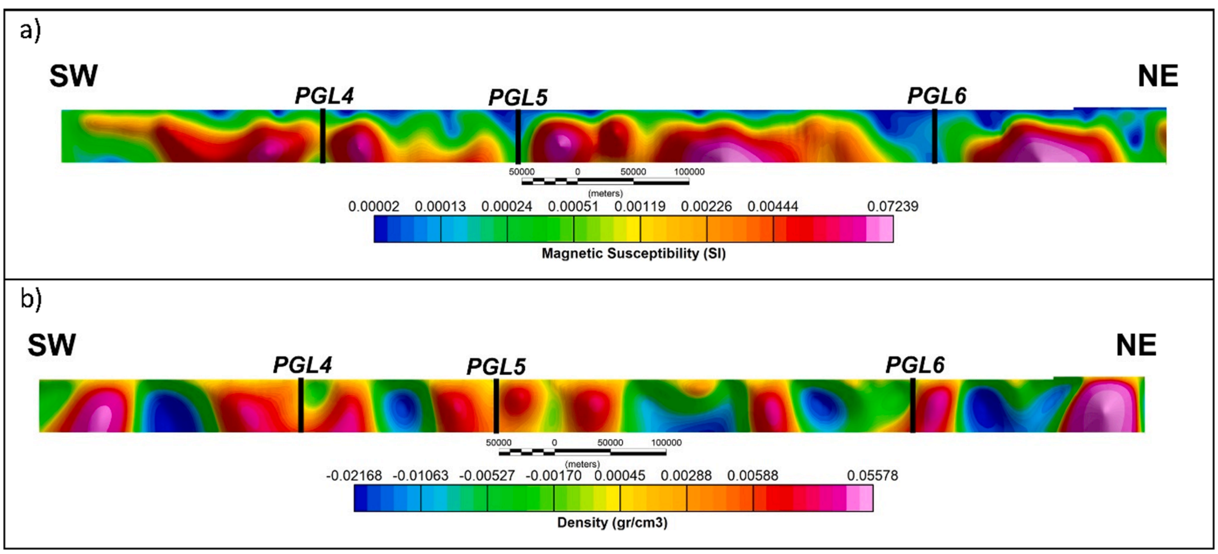

Fig. 6. Section 1: cross sections of Magnetic susceptibility (a) and Density (b) models. Black lines show the location of the primary geophysical structures interpreted.

province, a juvenile magmatic arc constructed predominant by emplacement and differentiation of mantle-derived magmas.

This domain is interpreted as the NW portion of the Ventuari-Tapajós Province (Tassinari and Macambira, 1999; Ibañez-Mejia and Cordani, 2020) or the Trans-Amazonian basement against which Rio Negro Belt were accreted (Kroonenberg, 2019, Bonilla et al., 2021). In the Geological Map of South America (Gómez et al., 2019) the basement rocks located in this domain are presented as older (2.05–1.6 Ga) than those to the west (1.8–1.4 Ga), so the PGL6 can be interpreted as the boundary/suture between the Ventuari-Tapajós and Rio Negro-Juruena geochronological provinces as presented by Ibañez-Mejia and Cordani (2020) and Bonilla et al. (2021).

5.2. Atabapo Belt (Rio Negro-Juruena tectonic domain)

This domain is located between PGL5 and PGL6 and shows secondary geophysical structures with two main trends (NNE-SSW and E-W) that do not seem to continue into neighboring tectonic domains. Basement exposures pertaining to this domain are observed in the SE portion of the region, along the border between Colombia and Brazil, and correspond to the late-Paleoproterozoic Mitú Complex. This domain corresponds to the broader geochronological province of Rio Negro-Juruena (Tassinari and Macambira, 1999) or Rio Negro Belt (Kroonenberg, 2019), which locally has been associated with the 1.8–1.74 Ga Atabapo Belt (Cordani et al., 2016a; Ibañez-Mejia and Cordani, 2020).

The PGL5, which limits this tectonic domain to the S-SW, is correlated with NW-SE regional features recognized by Cordani et al. (2010) and that these authors suggested represent intra-cratonic tectonic events responsible for regional heating and associated resetting of mica K-Ar ages and other isotope systems (e.g., Rb-Sr). Also, PGL5 can be interpreted as the possible limit between the Atabapo and Vaupés magmatic belts of Ibañez-Mejia and Cordani (2020). We provide a supplementary Figure (S2) with the location of these geological features and its relationship with PGL5.

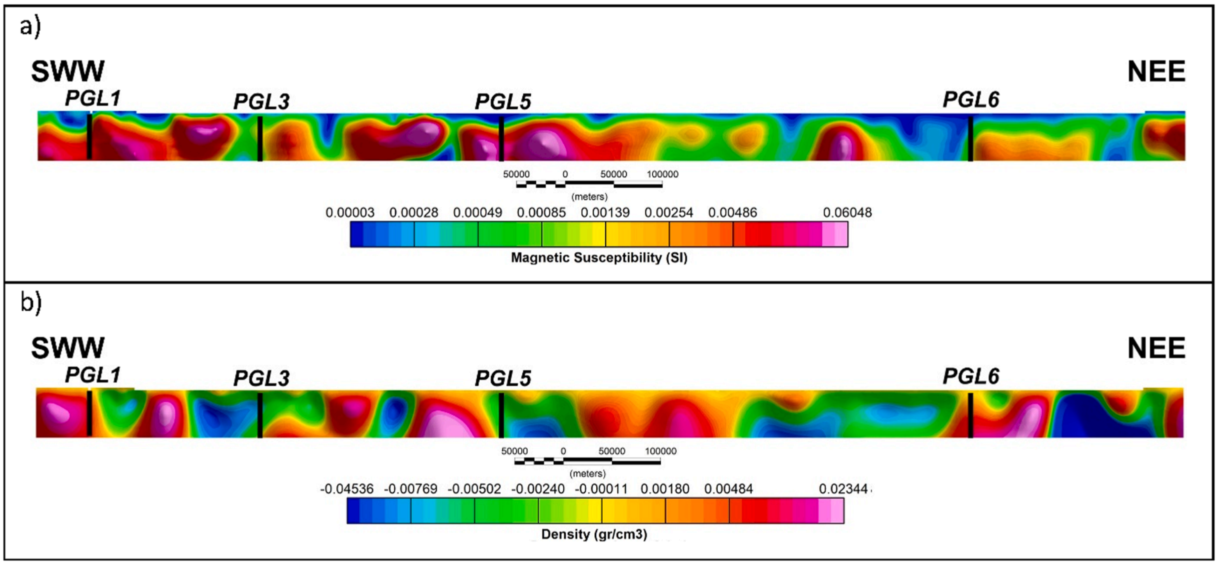

Fig. 7. Section 2: cross sections of Magnetic susceptibility (a) and Density (b) models. Black lines show the location of the primary geophysical structures interpreted.

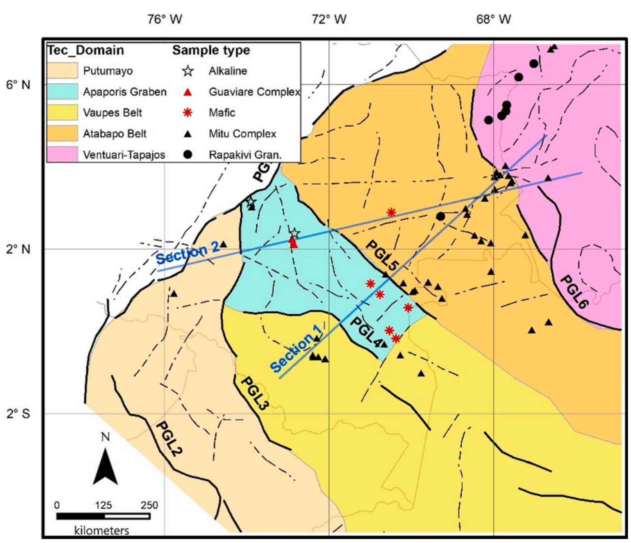

Fig. 8. Tectonic domains identified from geophysical/geological data integration and geochronological data.

5.3. Vaupés Belt (Rio Negro-Juruena tectonic domain)

Located to the south of the Atabapo Belt tectonic domain, and trending roughly parallel to it, lies the Vaupes Belt tectonic domain located between PGL3 and PGL5. The basement of this domain is exposed in isolated regions near its northern portion in the Araracuara range and the Vaupes region along the border between Colombia and Brazil. Although rocks in this tectonic domain are identified as part of the late-Proterozoic Mitú Complex by Gómez et al. (2015), Cordani et al. (2016a) and Ibañez-Mejia and Cordani (2020) proposed the existence of a younger magmatic belt in the Rio Negro-Juruena geochronological province (Vaupés Belt; 1.58–1.5 Ga) that likely accreted onto an already cratonized Atabapo Belt. The rough location of the boundary between those belts, as proposed by Ibañez-Mejia and Cordani (2020) on the basis of existing geochronologic data, is coherent with the PGL5 that separates the Atabapo and Vaupés belt tectonic domains we propose here.

Ibañez-Mejia and Cordani (2020) suggest that the geological evolution of the NW portion of the Amazonian Craton in Colombia exhibits some differences with respect to its SW portion in Brazil and Bolivia. These authors, however, recognize a progressive younging of basement domains towards the SW, and the presence of important magmatic episodes related to the Atabapo and Vaupés belts. In the present work, the names Atabapo and Vaupés Belt proposed by Cordani et al. (2016a) and Ibañez-Mejia and Cordani (2020) as subdivisions within the Rio Negro-Juruena province are utilized because they correlate well with the geophysical domains we interpret. It is important to note also that basement rocks in the Araracuara region (Fig. 1b) represent the westernmost exposures of the Amazonian Craton yet identified that to date do not show evidence of metamorphism associated with the Putumayo Orogen (Ibañez-Mejia et al., 2011).

5.4. Apaporis Graben tectonic domain

Located in between the Atabapo and Vaupés tectonic domains, and exhibiting a wedge-like or triangular shape, is the Apaporis Graben domain. This domain is characterized by a NW-SE magnetic low limited primarily by PGLs 1, 3, 4 and 5. We calculate the horizontal gradient of the reduction to magnetic pole (RTP) of the high-resolution magnetic data (see Fig. 3c) and identify, inside the regional magnetic low, linear magnetic features that run sub-parallel and orthogonal to the primary structure (Fig. 9). These features suggest that this domain represents a sedimentary basin filled by low susceptibility sediments and magnetic dike-like structures and other features that can be associated with tectonic extension during rifting. Some of these dike-like features were mapped by Etayo et al., (1986) as (1.2–1 Ga Rb/Sr) Mafic Vulcanites (Fig. 9) and Mafic dikes (Galvis et al., 1979). The Vaupés-1 well also drilled more than 1,500 m of Mesoproterozoic sandstones, intruded by a Neoproterozoic (826 Ma K/Ar) Gabbro (Kroonenberg, 2019). The Piraparaná Formation, that outcrops at the eastern limit of this domain and shows a westward dipping trend, is interpreted here as part of the volcano-sedimentary infill of this basin.

In the westernmost end of this tectonic domain (limited by PSG1 and PSG3), Ibañez-Mejia et al. (2011) obtained an U-Pb age of 1461 ± 10 Ma for the cratonic basement of the Serranía de la Macarena range. To the west of PGL3, Ibañez-Mejia et al. (2011) also identified a major Stenian-Tonian metamorphic event and proposed the name of Putumayo Orogen to describe it. Rocks of the Serranía de la Macarena and Araracuara ranges do not show, at least to this date, evidence of Putumayo-age metamorphism, and so the PGL3 is interpreted here as the eastern boundary for the influence of the Putumayo orogenic event in the region.

Recent work by Amaya López et al. (2020) in the northern part of the

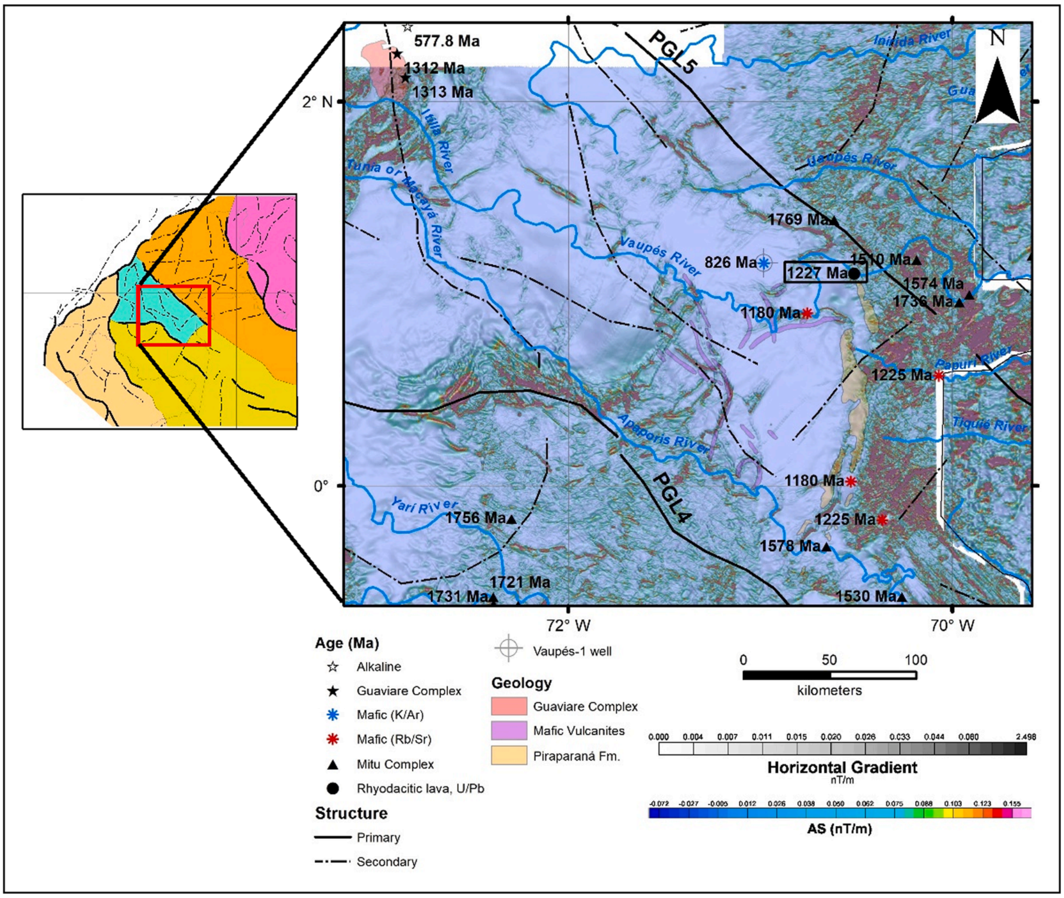

Fig. 9. "Apaporis Graben" tectonic domain. Geophysical structures and geological/geochronological elements (Etayo et al., 1986; Arango et al., 2011; Amaya López et al., 2020; Ibañez-Mejia and Cordani, 2020; Bonilla et al., 2020) superimposed to image of Horizontal gradient of the RTP magnetic field and Analytical signal of the total magnetic field anomaly (Moyano et al., 2018; ENCAL, 1988). Black rectangle highlights the location of the Yaca Yaca rhyodacitic lavas dated here using zircon U-Pb geochronology.

tectonic domain documented Mesoproterozoic (ca. 1.3 Ga) magmatism in the region, in a basement exposure they termed the 'Guaviare complex' (Figs. 1 and 8). According to Amaya López et al. (2020), the predominant lithologies in the Guaviare complex are quartz-feldspar gneises and quartzites (Termales Gneiss and La Rompida quartzite) and minor amphibolites (Unilla Amphibolite). Zircon U/Pb ages for the igneous protoliths of rocks of the Guaviare complex are $1312 \pm 5/11$ for Termales gneiss and $1313 \pm 8/12$ for Unilla Amphibolite. The youngest detrital age for La Rompida quartzite is 1238 ± 74 (similar to Termales gneiss and Unilla amphibolite) with peaks at 1500 Ma, 1730 Ma, and 2680 Ma.

The magmatism of the Guaviare Complex is clearly younger in age and isotopically distinct from older Atabapo and Vaupés belts to the east, but also slightly older than most of the Putumayo orogen basement to the west. Amaya López et al. (2020) indicated that the similarity in the maximum depositional age of the quartzites with the igneous age of the gneisses and amphibolite suggest that the latter contributed detrital material to nearby sedimentary basins. Also, these authors observed that zircon-age peaks at 1500 and 1730 Ma in metasediments correlate well with known basement ages in the Vaupés and Atabapo belts. Finally, the authors suggested that the Guaviare Complex formed in an extensional arc environment, possibly as part of a back-arc developed during the subduction and magmatic arc-development phase that characterizes the early stages of the Putumayo orogenic cycle. The age of metamorphism for the metaigneous and metasedimentary rocks of the Guaviare Complex, however, has not been determined.

This tectonic domain identified from our inversion of geophysical data correlates well with the previously identified 'Apaporis Rift' structure of Etayo et al. (1983) or the 'Guejar Impactogen' of Cediel (2019) (see Fig. 2 for comparison), although the limits and extension evidenced with the geophysical interpretation are clearly different. It is important to mention that this tectonic domain includes most of the geological evidence of younger (i.e., post-Putumayo) magmatism (Serranía de la Macarena, Guaviare Complex, Mafic intrusives and dikes, Vaupés-1 well) that have been recognized in the NW Amazonian Craton. We speculate that this domain originally developed as in intra-continental extensional structure (graben) within the Amazonian Craton prior to the formation of the Rodinia supercontinent. At its inception, this structure would have been associated with advancing subduction zones during the earliest (extensional) period of the Putumayo Orogenic cycle (e.g., Ibañez-Mejia et al., 2011; Cawood and Pisarevsky, 2017; Ibañez-Mejia, 2020), but later these structures may have been re-activated during the Putumayo collisional phase and the break-up of Rodinia in the late Neoproterozoic.

5.5. Putumayo tectonic domain

This domain is located at the SW end of our study area, south of PSG3 and east of PSG1. The only Information about craton-related rocks is provided in the works of Ibañez-Mejia et al. (2011, 2015, 2018) (Figs. 8 and 10). These authors studied cores from wells that drilled into the basement of the Putumayo basin, and identified Rio Negro-Juruena–like basement affected by Stenian-Tonian metamorphism for which they proposed the name of Putumayo Orogenic cycle (1.45–0.98 Ga) for this area. The recent works of Ibañez-Mejia and Cordani (2020) and Ibañez-Mejia (2020) provide recent reviews of the available geologic evidence

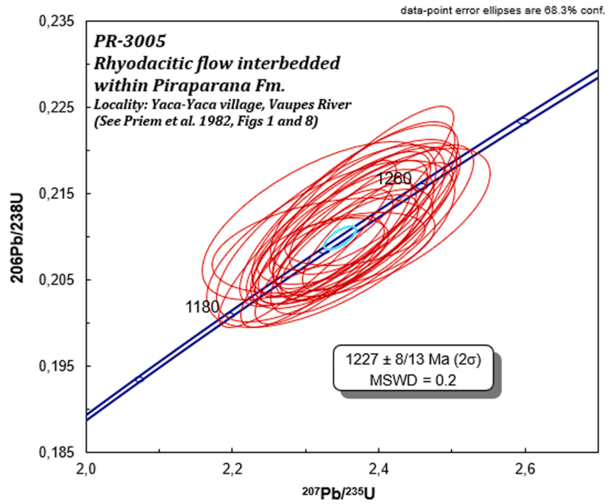

Fig. 10. U-Pb concordia diagram for sample PR-3005 of Priem et al. (1982).

to conclude that the Putumayo Province, and in general the NW portion of the Amazonian Craton, have a different geological and tectonic history compared to the SW portion of the Craton, where the Rondonia-San Ignacio and Sunsás geochronological provinces were originally defined (Tassinari and Macambira, 1999).Fig. 11..

The PGL2 structure, however, is close to the SW border of our study area, so its interpretation requires further investigation and integration with geological data to the west of this feature once it becomes available.

6. New U-Pb geochronological data on Apaporis Graben tectonic domain

Of all the tectonic domains discussed throughout this study, the evolution of the Apaporis Graben domain is arguably the most poorly known. To better understand the temporal history of extension along the Apaporis Graben, a sample from the Yaca-Yaca rhyodaciytic lavas unit, interpreted by Galvis et al. (1979) as the base of the Piraparaná formation (black rectangle, Fig. 9), was dated here using zircon U-Pb. The analysis performed were all concordant and yield a calculated $^{207}Pb/^{206}Pb$ weighted mean age of 1227 ± 8/13 Ma (Fig. 10). Analytical results are included as supplementary Table (ST2).

It is worth noting that Priem et al. (1982) reported a whole rock Rb-Sr age of 920 ± 90 Ma for these rhyodacitic lavas. However, the isochron age obtained by Priem et al. (1982) was based on a regression through multiple whole-rock aliquots obtained from different outcrops of this unit, and had a low goodness of fit (i.e., MSWD = 4.4). Based on a high initial $^{87}Sr/^{86}Sr$ ratio of 0.705 and using Rb-Sr model age calculations, these authors suggested that an extrusion age ca. 1110–1220 Ma for the rhyodacitic lavas was possible. However, due to the absence of a 920 Ma metamorphic event in the surrounding basement rocks, these authors concluded that isotopic rehomogenization due to metamorphism at this time was unlikely, and thus favored the 920 ± 90 Ma isochron fit as the age of eruption. The high initial $^{87}Sr/^{86}Sr$ ratio was interpreted to reflect incorporation of radiogenic strontium derived from older crustal material.

The new U-Pb zircon crystallization age obtained here clearly demonstrates that the Yaca-Yaca lavas, and hence the Piraparaná Formation, are significantly older than previously thought, and that in fact pre-date the collisional phase of the Putumayo Orogenic cycle (ca. 990 Ma) by ca. 240 Myr instead of post-dating it. Considering that the Piraparaná Formation forms the base of the graben-fill sediments associated with the Apaporis domain, our new geochronologic results allow us to conclude that crustal extension along the Apaporis Graben tectonic domain (Fig. 9) began at least in the late-Mesoproterozoic, thus entirely transforming its tectonic significance.

7. Discussion

The geophysical interpretation approach presented here, not applied to this area before, allowed us to identify six primary geophysical lineaments, which we interpret as representing possible crustal boundaries. Orientation and truncation between these major structures, combined with the distribution of secondary geophysical features, lends further evidence that these structures represent boundaries between geophysical domains, interpreted here as tectonic blocks with contrasting geologic histories. 3D inversion modelling of density and magnetic susceptibility (MVI) along selected profiles (Figs. 6 and 7) evidenced the deep crustal penetrating character of these primary structures. 3D models also allowed us to identify sources with different density/magnetic susceptibility that probably reflect variations in the petrologic nature and/or composition of the upper crust in this region.

Based on our geophysical interpretations, integrated with the available geological, geochronologic and isotopic information, five tectonic domains, each one with characteristic geophysical and geological features, were proposed: Ventuari-Tapajós, Atabapo Belt, Vaupés Belt, Apaporis Graben and Putumayo (Fig. 8). Schematic geological cross-sections across the sections used for the geophysical data interpretation (Figs. 6 and 7) are presented in Fig. 10.

According to the available geological and geochronological data, and the new tectonic framework proposed in the present work, the salient features of the geological evolution for the area can be summarized as follows:

- Formation of the Ventuari-Tapajós basement domain, against which a younger magmatic arc (Atabapo belt) was accreted, leaving behind a suture interpreted here as the PGL6. We propose the name 'Atabapo Suture' for our PGL6 (Fig. 12a).

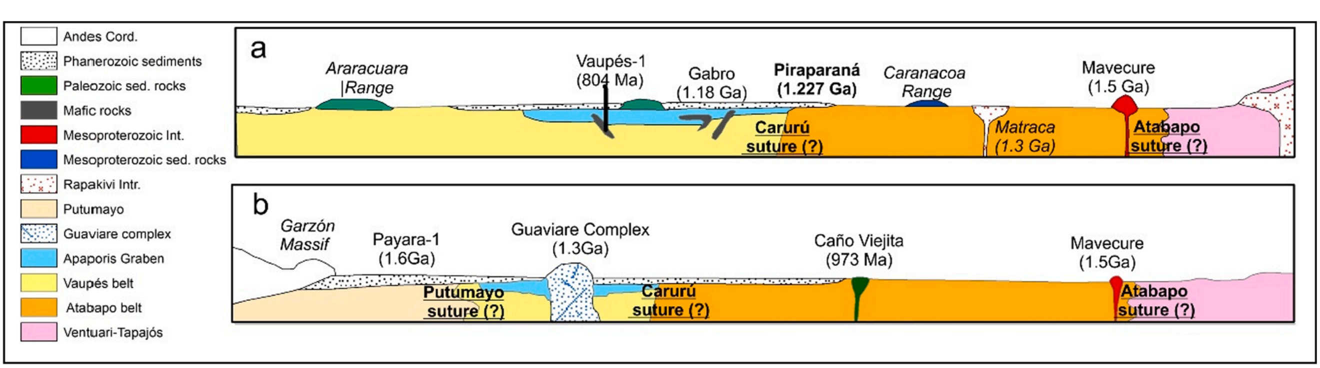

Fig. 11. Schematic geological cross sections: 1 (a) and 2 (b).

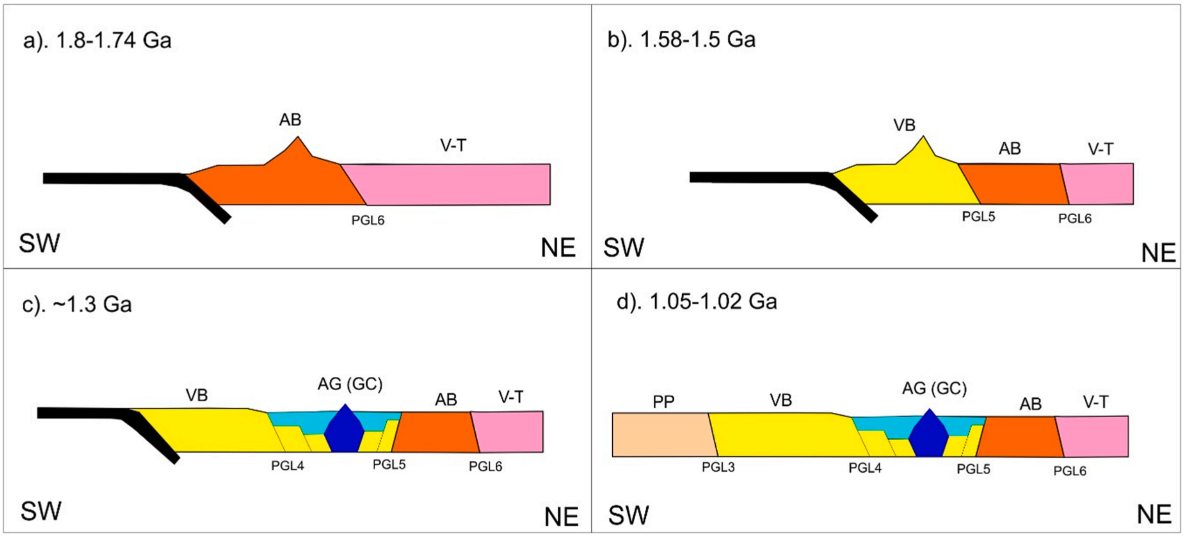

Fig. 12. Sketch models for the tectonic evolution for NW Amazonian Craton (see details in text). V-T: Ventuari-Tapajós; AB: Atabapo Belt; VB: Vaupés Belt; AR(GC): Apaporis Graben (Guaviare Complex); PP: Putumayo Province. PGL: Primary geophysical lineament.

- Later accretion of a younger magmatic belt (Vaupés belt) against the already cratonized Atabapo Belt (Cordani et al., 2016a) along the PGL5. Our PGL5 coincides with the location and trend of the Carurú fault, and thus we propose the name of Carurú Suture for this boundary (Fig. 12b).
- An early extensional phase (Apaporis Graben) possibly associated with back-arc opening during the early stages of the Putumayo Orogenic cycle, that affected the Vaupés (and Atabapo?) belts. This tectonic domain is characterized by a late Mesoproterozoic basin infill with an important volcanic component (i.e., Piraparaná Fm.) cross-cut by Neoproterozoic mafic intrusives. Some of these extensional structures might have been reactivated during post-Putumayo times (i.e., Rodinia breakup), leading to Neoproterozoic alkalic magmatism such as the syenites documented in the Guaviare Complex (Amaya López et al., 2021) (Fig. 12c).
- Terrain accretion and high-grade metamorphism associated with the compressional stages of the Putumayo Orogeny. Effects of this metamorphism have not yet been documented to the east of the PGL3, which suggests this boundary may correspond to the Putumayo structural limit or possibly even its suture. This proposed boundary also appears to offset the PGL4 that bounds Apaporis Graben structure to the S, providing additional evidence that the Apaporis Graben indeed pre-dates Putumayo collision and that it became active in the mid Mesoproterozoic (Fig. 12d).
- Phanerozoic evolution of the NW portion of the Amazonian Craton produced the PGL1 that crosscuts all the other (older) terrane boundaries mentioned above. This PGL1 currently coincides with the Andean deformation front in the south of our study area (i.e., in the Putumayo Basin), but to the north, underneath the Llanos Basin, can potentially represent the northwesternmost limit of the Guiana shield.

8. Conclusion

The gravimetric and magnetometric data available for eastern Colombia was interpreted qualitatively and quantitatively, showing significant variations and lateral contrasts in the physical properties (density, magnetic susceptibility) of the NW Amazonian Craton. These lateral variations reveal the structural/tectonic features in a level of detail not available before and not registered in existing regional maps and tectonic models.

Multiscale edge detection was applied for the first time to the study area, which allowed the identification of six main geophysical lineaments. We interpreted these lineaments as possible crustal boundaries between different geophysical domains, and use them here to better outline tectonic domains previously identified using geochronology but whose boundaries remained only loosely constrained due to the sparse nature of the geochronologic data.

From the integrated interpretation of geophysical, geological, geochronological, and isotopic information, we propose a geological-geophysical model for the Amazonian Craton formed by five tectonic domains: Ventuari-Tapajós, Atabapo Belt, Vaupés Belt, Apaporis Graben and Putumayo orogen. Each one of the domains has its geophysical and geological characteristics, which in turn allows inferring the tectonic significance of our identified geophysical boundaries within the framework of the W Guiana Shield geology.

This study: i) provides the first regional reconstruction of crustal-scale structural features in NW South America; ii) significantly improves our understanding of the regional tectonic architecture of the NW Amazonian Craton using geophysical potential field methods; and iii) provides a testable tectonic framework that can guide future field and geochronologic research in this region. For example, the precise location of PGL6 and PGL5 as provided from our inversion of the geophysical data (Fig. 8), can be utilized to design future field and geochronologic campaigns aimed at better understanding the nature of these boundaries and evaluating whether they in fact represent crustal-scale structural limits (i.e., our hypothesized Atabapo and Carurú sutures).

Although the interpretation of the geophysical limits identified here is in excellent agreement with previously suggested boundaries that had only been loosely constrained using geochronologic information, our geophysical/structural model allows tracing the location of these limits more accurately. Nevertheless, further field and geochronologic work must be done to continue evaluating the tectonic significance of the structural boundaries and domains proposed here, and better determine their role in the construction and stabilization of the NW South American continental platform.

CRediT authorship contribution statement

Ismael E. Moyano-Nieto: Conceptualization, Methodology, Investigation, Writing – original draft. **Germán A. Prieto:** Supervision, Writing – review & editing. **Mauricio Ibañez-Mejia:** Investigation, Writing – review & editing.

Declaration of Competing Interest

The authors declare that they have no known competing financial interests or personal relationships that could have appeared to influence the work reported in this paper.

Acknowledgements

The authors want to acknowledge the Departamento de Geociencias at Universidad Nacional de Colombia and the Servicio Geológico Colombiano for the support and collaboration in the present study as a part of the PhD in geosciences thesis of the first author. We also would like thank Dr. Moacir Macambira and other anonymous reviewer for their suggestions and recommendations that helped improve this contribution.

Appendix A. Supplementary material

Supplementary data to this article can be found online at https://doi.org/10.1016/j.precamres.2022.106735.

References

Almeida, F.F.M. de, Hasui, Y., Brito Neves, B.B., Fuck, R.A., 1981. Brazilian Structural Provinces: An Introduction. Earth Sci. Rev. 1981, 17, 1–29.

Amaya López, C., Restrepo Álvarez, J.J., Weber Scharff, M., Cuadros Jiménez, F.A., Botelho, N.F., Ibáñez Mejía, M., Maya Sánchez, M., Pérez Parra, O.M., Ramírez Cárdenas, C., 2020. The Guaviare Complex: new evidence of Mesoproterozoic (ca. 1.3 Ga) crust in the Colombian Amazonian Craton. Boletín Geológico 47, 5–34.

Amaya López, C., Weber Scharff, M., Ibáñez Mejía, M., Cuadros Jiménez, F.A., Restrepo Álvarez, J.J., Botelho, N.F., Maya Sánchez, M., Pérez Parra, O.M., Ramírez Cárdenas, C., 2021. San José de Guaviare Syenite, Colombia: Repeated Ediacaran intrusions in the northwestern Amazonian Craton. Boletin Geologico 48 (1), 49–79.

Arango, M., Nivia, A., Zapata, G., Giraldo, M., Bermúdez, J., Albarracín, H., 2011. Geología y geoquímica de la Plancha 350 San José del Guaviare. Servicio Geológico Colombiano. pp 165.

Barrios, F., Cordani, U., Kawashita, K., 1985. Caracterización geocronológica del Territorio Federal de Amazonas, Venezuela. Memorias VI Congreso Geológico Venezolano. Tomo III, 1432-1480.

Bettencourt, J.S., Leite Jr., W.B., Ruiz, A.S., Matos, R., Payolla, B.L., Tosdal, R.M., 2010. The Rondonian-San Ignacio Province in the SW Amazonian Craton: an overview. J. South Am. Earth Sci. 29 (1), 28–46. https://doi.org/10.1016/j.jsames.2009.08.006.

Blakely, R., Simpson, R., 1986. Approximating edges of source bodies from magnetic or gravity anomalies. Geophysics. I (7), 1494–1498.

Bonilla-Perez, A., Frantz, J.C., Charão-Marques, J., Cramer, T., Franco-Victoria, J.A., Mulocher, E., Amaya-Perea, Z., 2013. Petrografía, Geoquímica y Geocronología del Granito de Parguaza en Colombia. Boletin de Geología 35 (2), 83–104. https://doi.org/10.18273/revbol.

Bonilla, A., Franco, J., Cramer, T., Poujol, M., Cogné, N., Nachtergaele, S., De Gravé, J., 2020. Apatite LA-ICP-MS U-Pb and fission-track geochronology of the Caño Viejita gabbro in E-Colombia: Evidence for Grenvillian intraplate rifting and Jurassic exhumation in the NW Amazonian Craton. J. South Am. Earth Sci. 98, 102438 https://doi.org/10.1016/j.jsames.2019.102438.

Bonilla, A., Cramer, T., De Grave, J., Alessio, B., Glorie, S., Kroonenberg, S., 2021. (2021) The NW Amazonian Craton in Guainía and Vaupes departments, Colombia: Transition between orogenic to anorogenic environments during the Paleo-Mesoproterozoic. Precambr. Res. 360, 106223 https://doi.org/10.1016/j.precamres.2021.106223.

Brito, B., 2011. The Paleoproterozoic in the South American continent: diversity in the geologic time. J. South Am. Earth Sci. 32, 270–286.

Buchely, F., Gómez, L., Buitrago, J., Cristancho, A., Moreno, M., Hincapié, G., Aranzazu, J., Castelblanco, E., Ceballos, L., Quiñonez, C., Zafra, M., 2015. Elaboración de la cartografía geológica de un conjunto de planchas a escala 1: 100.000 ubicadas en cuatro bloques del territorio nacional identificados por el Servicio Geológico Colombiano Grupo 2: zonas Sur A y Sur B. In: Geología de la Plancha 305 San Juan de Arama. Memoria Explicativa. Servicio Geológico Colombiano, p. 121.

Cawood, P., Pisarevsky, S., 2017. Laurentia-Baltica-Amazonia relations during Rodinia assembly. Precambrian Res. 292, 386–397. https://doi.org/10.1016/j.precamres.2017.01.031.

Cediel, F., 2019. Phanerozoic Orogens of Northwestern South America: Cordilleran-Type Orogens. Taphrogenic Tectonics. The Maracaibo Orogenic Float. The Chocó-Panamá Indenter. In: Cediel F., Shaw R. (Ed.), Geology and Tectonics of Northwestern South America. The Pacific-Caribbean-Andean Junction (pp 3-95). Switzerland. Springer.

Celada C., Garzón M., Gómez E., Khurama S., López J., Mora M., Navas O., Pérez R., Vargas O., Westerhof A., 2006. Potencial de recursos minerales en el Oriente colombiano: compilación y análisis de la información geológica disponible fase 0 versión 1.0. Ingeominas, 233 pp.

Cordani, U., Teixeira, W., 2007. Proterozoic accretionary belts in the Amazonian Craton. In: Hatcher Jr, R.D., Carlson, M.P., McBride, J.H. & Martínez–Catalá, J.R. (editors), 4–D Framework of continental crust. Geological Society of America, Memoir 200, p. 297–320. https://doi.org/10.1130/2007.1200(14).

Cordani, U.G., Teixeira, W., D'agrella-Filho, M.S., Trindade, R.I., 2009. The position of the Amazonian Craton in supercontinents. Gondwana Research 15, 396–407. https://doi.org/10.1016/j.gr.2008.12.005.

Cordani, U., Fraga, L., Reis, N., Tassinari, C., Brito-Neves, B., 2010. On the origin and tectonic significance of the intra-plate events of Grenvillian-type age in South America: a discussion. J. South Am. Earth Sci. 29 (2010), 143–159.

Cordani, U.G., Sato, K., Sproessner, W., Fernandes, F.S., 2016a. U-Pb zircon ages of rocks from the Amazonas Territory of Colombia and their bearing on the tectonic history of the NW sector of the Amazonian Craton. Braz. J. Geol. 46 (suppl 1), 5–35.

Cordani U., Ramos, V., Fraga, L., Cegarra, M., Delgado, I., De Souza, K., Gomes, F & Shobbenhaus, C. (2016b). Explanatory notes: Tectonic Map of South America. Second edition, scale 1:5 000 000. Commission for the geological map of the World. Paris, France, ISBN 978-2-917310-26-7. DOI: 10.14682/2016TEMSA.

Crawford, B., Betts, P., Ailleres, L., 2010. A potential field approach to defining major lithospheric structures along the margin of the west Australian craton. ASEG Extended Abstracts 2010 (1), 1–4.

De Boorder, H., 1981. Structural-geological interpretation of SLAR imagery of the Colombian Amazones. Trans. Inst. Min. Metall. 90, B145–B152.

De Boorder, H., 2019. The La Trampa wedge (SE Colombia) revisited. 11th Inter Guiana Geological Conference.

De Castro, D.L., Fuck, R.A., Phillips, J.D., Vidotti, R.M., Bezerra, F.H.R., Dantas, E.L., 2014. Crustal structure beneath the Paleozoic Parnaíba Basin revealed by airborne gravity and magnetic data, Brazil. Tectonophysics 614, 128–145. https://doi.org/10.1016/j.tecto.2013.12.009.

Dentith, M., Mudge, S., 2014. Geophysics for the Mineral Exploration Geoscientist. Cambridge University Press, United Kingdom.

ENCAL, S.A., 1988. Projeto Extremo Noroeste do Brasil (Levantamento Aeromagnético e Aerogamaespectrométrico). Fase II 7.

Etayo, F., Barrero, D., Lozano, H., Espinoza, A., González, H., Orrego, A., Ballesteros, I., Forero, H., Ramírez, C., Zambrano, F., Duque-Caro, H., Vargas, R., Nuñez, A., Alvarez, J., Ropaín, C., Cardozo, E., Galvis, N., Sarmiento, L., Albers, J., Case, J., Greenwood, W., Singer, R., Berger, B., Cox, D., Hodges, C., 1983. Mapa de Terrenos Geológicos de Colombia. Publ. Geol. Esp. INGEOMINAS, pp 139.

Etayo, F., Buenaventura, J., Vargas, R., Espinosa, A., Nuñez, A., González, H., Orrego, A., 1986. Mapa Geológico de Colombia, scale 1:1'000,000. INGEOMINAS, Bogotá.

Fitzgerald, D., Milligan, P., 2013. Defining a deep fault network for Australia, using 3D "worming". SEG 2013 Annual Meeting. Houston.

Förste, C., Bruinsma, S., Abrikosov, O., Lemoine, J., Marty, J., Flechtner, F., Balmino, G., Barthelmes, F., Biancale, R., 2014. EIGEN-6C4: The latest combined global gravity field model including GOCE data up to degree and order 2190 of GFZ Potsdam and GRGS Toulouse. GFZ Data Services. https://doi.org/10.5880/icgem.2015.1.

Galvis, J., Huguett, A., Ruge, P., De Boorder, H., 1979. Mapa Geológico de la Amazonia Colombiana. Scale 1:500.000. Proyecto Radargramétrico del Amazonas. Bogotá.

Gómez, J., Montes, N., Nivia, A., Diederix, H., compiladores, 2015. Atlas Geológico de Colombia 2015. Escala 1:500 000. Servicio Geológico Colombiano. Bogotá.

Gómez, J., Schobbenhaus, C., Montes, N., compilers, 2019. Geological Map of South America 2019. Scale 1:5 000 000. Commission for the Geological Map of the World (CGMW), Colombian Geological Survey and Geological Survey of Brazil. Paris.

Graterol, V, Vargas, A., 2010. Mapa de Anomalía de Intensidad Magnética Total y de Intensidad Magnética Total Reducida al Polo de la República de Colombia y Mapa de Anomalía de Bouguer total de la República de Colombia. Agencia Nacional de Hidrocarburos (ANH).

Hackley, P., Urbani, F., Karlsen, A., Garrity, C., 2005. Geologic shaded relief map of Venezuela. USGS Open-file report 2005–11038.

Heath, P., Dhu, T., Reed, G., Fairclough, M., 2009. Geophysical modelling of the Gawler Craton, SA - interpreting geophysics with geology. ASEG Extended Abstracts 2009 (1), 1.

Horowitz, F., Strykowski, G., Boschetti, F., Hornby, P., Archibald, N., Holden, D., Ketelaar, P., Woodcock, R., 2000. Earthworms; "multiscale" edges in the EGM96 global gravity field. SEG expanded abstracts. Alberta, Canadá.

Ibañez-Mejia, M., Gehrels, G.E., Ruiz, J., Vervoort, J.D., Eddy, M.E., Li, C., 2014. Small-volume baddeleyite (ZrO2) U-Pb geochronology and Lu–Hf isotope geochemistry by LA-ICP-MS. Techniques and applications. Chem. Geol. 384, 149–167. https://doi.org/10.1016/j.chemgeo.2014.07.011.

Ibañez-Mejia, M., Pullen, A., Arenstein, J., Gehrels, G.E., Valley, J., Ducea, M.N., Mora, A.R., Pecha, M., Ruiz, J., 2015. Unraveling crustal growth and reworking processes in complex zircons from orogenic lower–crust: the Proterozoic Putumayo Orogen of Amazonia. Precambr. Res. 267, 285–310. https://doi.org/10.1016/j.precamres.2015.06.014.

Ibañez-Mejia, M., Bloch, E.M., Vervoort, J.D., 2018. Timescales of collisional metamorphism from Sm-Nd, Lu-Hf and U-Pb thermochronology: a case from the Proterozoic Putumayo Orogen of Amazonia. Geochimica Et Cosmochimica Acta 235, 103–126. https://doi.org/10.1016/j.gca.2018.05.017.

Ibañez-Mejia, M., 2020. The Putumayo Orogen of Amazonia: A synthesis. In J. Gomez & D. Mateus-Zabala (Eds.), The Geology of Colombia (Vol. 1, pp. 101–131). Bogotá: Servicio Geológico Colombiano. http://doi.org/10.32685/pub.esp.35.2019.06.

Ibañez–Mejia, M., Cordani, U.G., 2020. Zircon U–Pb geochronology and Hf–Nd–O isotope geochemistry of the Paleo– to Mesoproterozoic basement in the westernmost Guiana Shield. In: Gómez, J., Mateus–Zabala, D. (editors), The Geology of Colombia, Volume 1 Proterozoic – Paleozoic. Servicio Geológico Colombiano, Publicaciones Geológicas Especiales 35, p. 65–90. Bogotá. https://doi.org/10.32685/pub.esp.35.2019.04.

Isles, D., Rankin, L., 2013. Geological Interpretation of Aeromagnetic Data. Australian Society of Exploration Geophysicists. CSIRO, Perth, Australia, 365 pp.
Jacoby, W., Smilde, P., 2009. Gravity Interpretation: Fundamentals and Application of Gravity Inversion and Geological Interpretation. Springer,-Verlag, Berlín, 395 pp. ISBN: 978-3-540-85328-2.
Ibañez-Mejia, M., Ruiz, J., Valencia, V.A., Cardona, A., Gehrels, G.E., Mora, A.R., 2011. The Putumayo Orogen of Amazonia and its implications for Rodinia reconstructions: new U-Pb geochronological insights into the Proterozoic tectonic evolution of Northwestern South America. Precambr. Res. 191 (1–2), 58–77.
Kroonenberg, S., Reeves, C., 2012. Geology and petroleum potential, Vaupés-Amazonas Basin, Colombia. In: Cediel, F. (Ed.), Petroleum Geology of Colombia, 15. Universidad EAFIT, Medellín, p. 92.
Kroonemberg, S., De Roever E., 2010. Geological Evolution of the Amazonian Craton, in: Amazonia, Landscape and Species Evolution. Edited by C. Hoorn and F Wesselingh. Wiley, p. 9-28.
Kroonemberg, S., 2019. The Proterozoic Basement of the Western Guiana Shield and the Northern Andes. In: Cediel F., Shaw R. (Ed.), Geology and Tectonics of Northwestern South America. The Pacific-Caribbean-Andean Junction (pp 115-192). Switzerland. Springer.
Li, Y., Melo, A., Martinez, C., Sun, J., 2019. Geology differentiation: a new frontier in quantitative geophysical interpretation in mineral exploration. The Leading Edge 38 (1), 60–66.
López J., Mora B., Jiménez D., Khurama S., Marín E., Obando G., Páez T., Carrillo L., Bernal V., Celada C., 2010. Cartografía geológica y muestreo geoquímico de las Planchas 297 – Puerto Inírida, 297 Bis – Merey Y 277 Bis – Amanaven, Departamento del Guainia. Ingeominas, Bogotá. 158 pp.
MacLeod, I., Ellis, R., 2013. Magnetic Vector Inversion, a simple approach to the challenge of varying direction of rock magnetization. ASEG-PESA 23rd International Geophysical Conference and Exhibition. Melbourne, Australia.
Meyer, B., Saltus, R., Chulliat, A., 2017. EMAG2: Earth Magnetic Anomaly Grid (2-arc-minute resolution) Version 3. National Centers for Environmental Information, NOAA. Model. doi: 10.7289/V5H70CVX.
Moyano, I., Lara, N., Ospina, D., Salamanca, A., Arias, H., Gómez, E., Puentes, M., Rojas, O., 2018. Mapa de anomalías Geofísicas de Colombia para Recursos Minerales, Versión 2018. Servicio Geológico Colombiano, Bogotá.
Moyano, I, Cordani, R., Cárdenas, L., Lara, N., Rojas, O, Puentes, M., Ospina, D., Salamanca, A., Prieto, G., 2020. Contribution of new airborne geophysical information to the geological knowledge of eastern Colombia. In: Gómez, J. & Mateus–Zabala, D. (editors), The Geology of Colombia, Volume 1 Proterozoic – Paleozoic. Servicio Geológico Colombiano, Publicaciones Geológicas Especiales 35, p. 17–36. Bogotá. https://doi.org/10.32685/pub.esp.35.2019.02.
Moyano, I., Prieto, G., 2021. Structural signatures of the Amazonian Craton in eastern Colombia from gravity and magnetometry data interpretation. Tectonophysics 800 (2021), 228705. https://doi.org/10.1016/j.tecto.2020.228705.
Pessano, P.C., Ganade, C.E., Tupinambá, M., Teixeira, W., 2021. Updated map of the mafic dike swarms of Brazil based on airborne geophysical data. J. South Am. Earth Sci. 107 (1–2), 103076 https://doi.org/10.1016/j.jsames.2020.103076.
Priem, H.N.A., Andriessen, P.A.M., Boelrijk, N.A.I.M., De Boorder, H., Hebeda, E.H., Huguett, A. et al., 1982. Geochronology of the precambrian in the Amazonas region of southwestern Colombia western Guiana shield. Geologie & Mijnbouw, 229–242.
Rodríguez, G., Sepúlveda, J., Ortiz, F., Ramírez, C., Ramos, K., Bermúdez, J., Sierra, M., 2010. Mapa Geológico Plancha 443 Mitú – Vaupés. Ingeominas.
Santos, J., Hartmann, L., Gaudette, H., Groves, D., Mcnaughton, N., Fletcher, I., 2000. A new understanding of the Provinces of the Amazonian craton based on integration of field mapping and U-Pb and Sm-Nd geochronology. Gondwana Res. 3 (4), 453–488.
Tassinari, C., Cordani, U.G., Nutman, A., van Schmus, W., Bettencourt, J.S., Taylor, P., 1996. Geochronological systematics on basement rocks from the Rio Negro-Juruena province (Amazonian Craton) and tectonic implications. Int. Geol. Rev. 38 (2), 161–175.
Tassinari, C., Macambira, M., 1999. Geological provinces of the Amazonían Craton. Episodes 22, 173–182.
Teixeira, W., Tassinari, C.C.G., Mondin, M., 2002. Características isotópicas (Nd e Sr) do plutonismo intrusivo no extremo NW do Cráton Amazônico, Venezuela, e implicações para a evolução paleoproterozóica. Geol. USP, Sér. cient. 2 (1), 131–141.
Teixeira, W., Geraldes, M.C., Matos, R., Ruiz, A.S., Saes, G., Vargas-Mattos, G., 2010. A review of the tectonic evolution of the Sunsás belt, SW Amazonian Craton. J. South Am. Earth Sci. 29 (1), 47–60. https://doi.org/10.1016/j.jsames.2009.09.007.
Yan, J., Lü, Q., Deng, Z., Meng, G., Liu, Y., Zhao, J., 2011. Gravity and magnetic multi-scale edge detection and its application on tectonic framework research of the lower and middle reaches of the Yangtze River metallogenic belt, China. International Workshop on Gravity, Electrical & Magnetic Methods and Their Applications. https://doi.org/10.1190/1.3659069.